Arab Journal of Nuclear Sciences and Applications

Web site: ajnsa.journals.ekb.eg

(E S N S A)

Study the Deuteron and Alpha-Particle Properties Applying Comparative Analyses

A. Amar

Department of Physics, Faculty of Science, Tanta University, Tanta 31527, Egypt

ARTICLE INFO

ABSTRACT

A comparison between deuteron and alpha particle, has been done from many aspects. Different comparative methods have been used to study alpha and deuteron properties. Diffraction model has been applied to deuteron and alpha particles. The radial region of sensitivity has been tested using the distance of the closest approach where Notch test was applied to study the sensitivity of the optical model parameters. The reaction cross section and reflexion coefficients η_L of the deuteron and alpha elastically scattered by light nuclei (^{6,7}Li, ^{9}Be and ^{11}B) have been used for the comparison between the two projectiles under consideration. The imaginary potentials for deuteron and alpha elastically scattered by ^{7}Li has been used also, to study the difference between alpha and the deuteron. It was observed that deuteron has a signature of halo properties.

1. INTRODUCTION

Deuteron and alpha nuclei are used as projectiles to examine the cluster structure of light nuclei. It is well-known that the light nuclei tend to form clusters, as in the case of ^{6}Li≡α+d, and ^{7}Li≡α+t, and ^{9}Be≡^{5}He+^{4}He [1]. Studying the light nuclei can help nuclear scientists to understand the structure of the nucleus and the mechanisms of nuclear reactions. The ^{6}Li(p,γ)^{7}Be reaction [2] could be used to interpret the abundance of ^{6}Li in the universe. As the reaction ^{6}Li(p,γ)^{7}Be takes place in the universe, the percent of ^{7}Be increases where ^{6}Li decreases. Obtaining information about the cluster structures of light nuclei, such as ^{6,7}Li, ^{7,9}Be and ^{10,11}B is still a rich field. In a contrast to α-particles, deuterons are loosely bound nuclei with a very low binding energy (2.22 - 2.42MeV) [3-4] with a deformed shape.

The scattering cross sections of weakly bound projectiles like deuterons are found to behave significantly differently than tightly bound projectiles like alpha [5]. The binding energy and angular momentum are responsible for the form of the wave function, which extends to very large radii in the case of weakly bound projectiles (deuterons) where the Schrodinger equation could be expressed as: $(E - \varepsilon_n - T_{aA}(R\alpha))\langle \phi_{bx}^n R\alpha \mid \Psi^{j_{in}(+)}\rangle - \sum_{\bar{\sigma}'} U_{\bar{\alpha},\bar{\alpha}'}(R)\langle \phi_{bx}^{n'} R\alpha' \mid \Psi^{j_{in}(+)}\rangle = 0$ where ε_n is the binding energy and α is the

orbital angular momentum [6]. The elastic scattering calculations of deuterons show that the total cross section is substantially higher than the calculated total cross section of alpha as a projectile on similar mass targets [7].

Even with the argument mentioned by Berezhnoy et al. 2005 [8], the situation cannot be explained as long range Van der Waals field. In the nucleus, nuclear field is governed by mesons with short range color force. The shape and binding energy of the deuteron and alpha nuclei produce an opportunity to compare them from different aspects such as cross section, reflection coefficient, breakup, and optical parameters. We expect that the low binding energy of deuterons (breakup) is responsible for the high calculated cross section observed in the case of deuterons elastically scattered by light nuclei. The experimental data used in the present work is available at the cited source [9].

In this work some properties of deuteron and alpha-particle using results in references [2] and [7] are studied. In these two papers, elastic scattering of deuteron and alpha-particles from a few light nuclei (^{6,7}Li, ^{9}Be and ^{11}B) are studying by means of optical model (OM).

2. RESULTS AND DISCUSSIONS

a. Diffraction model application to deuteron and alpha projectiles

The diffraction model use the following relation to calculate the radius of the nucleus [10]:

$$R = \frac{1.22\lambda}{2\sin(\theta)} \qquad (1)$$

where θ is the angle of the first minimum, $\lambda = \frac{h}{mv}$ is the de Broglie wave length and R is radius of the nucleus. We will apply this equation for deuteron and alpha for the ground and the excited states. For alpha as projectile:

$$R_{diff}(\alpha) = \frac{0.612\,h}{m_\alpha\,v_\alpha\sin(\theta_\alpha)}\ ,\ R_{diff}(\alpha) = \frac{0.612\,h}{\sqrt[2]{2\,E_\alpha m_\alpha}\,\sin(\theta_\alpha)} \quad (2)$$

The same form of equation (2) could be applied to the deuteron as a projectile. Where $E_\alpha(E_d)$, $m_\alpha(m_d)$ and $\Theta_\alpha(\Theta_d)$ are the incident energy of alpha (deuteron), mass of alpha (deuteron) and incident angle of alpha (deuteron), respectively. If we apply the equation (2) to the ground and first exited state of ^{6}Li, $R_{diff}(\alpha)$ should equal $R_{diff}(d)$. Thus, we can obtain:

$$\frac{0.612\,h}{m_\alpha\,v_\alpha\sin(\theta_\alpha)} = \frac{0.612\,h}{m_d\,v_d\sin(\theta_d)} \qquad (3)$$

Then, $\quad m_\alpha\,v_\alpha\sin(\theta_\alpha) = m_d\,v_d\sin(\theta_d) \qquad (4)$

Where $m_\alpha = 1.9772200 m_d$ [4]. Thus,   as approximation, we could take $m_\alpha \simeq 2m_d$. The value of $\theta_\alpha = \theta_d$, only if the incident energy (momentum) of alpha should be twice of the deuteron energy ($E_\alpha = 2E_d$). For deuteron (alpha)-target system, the relation between c.m. and laboratory system the relation could be used:

$$\frac{1}{2}m_d\left(v_{df}^{CM}\right)^2 + \frac{1}{2}\frac{m_d^2}{m_T}\left(v_{df}^{CM}\right)^2 = \frac{1}{2}\frac{m_d m_T}{m_d+m_T}\left(v_{di}^L\right)^2 \quad (5)$$
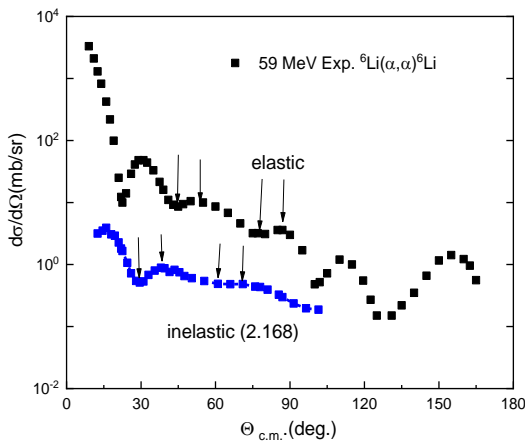
The same principle has been applied to d+^{11}B (^{12}C) and α+^{11}B (^{12}C) in the reference [10]. Deuteron and alpha elastic and inelastic scattering on ^{6}Li have been analyzed using the same principle at energies of 25 MeV and 59 MeV, respectively. Inelastic scattering data has been analyzed using the refraction model (RM) of the nucleus, which was developed for determining the radii of the excited states for both deuteron and alpha projectiles [10]. The root mean square (rms) radius R* of the excited state is calculated by subtracting the diffraction radii of the exited and ground states and applying the following expression:

$$R^* = R_0 + [R_{dif}^* - R_{dif}(0)] \qquad (6)$$

where R_0 is the rms of the ground state of the studied nucleus, and R^*_{dif} and $R_{dif}(0)$ are the diffraction radii determined from the positions of the minima and maxima of the experimental angular distributions of the elastic and inelastic scattering, respectively [10] **as shown in Figs. 1 and 2**. The difference R_{dif} (8.56) - R_{dif} (0.00) for d+^{11}B scattering obtained by us is 0.589 fm, which differs slightly from the literature, 0.46±0.30 fm. Applying equation (6) to the deuteron and alpha particles elastically scattered by ^{6}Li, we could calculate the root mean square (rms) radius $\langle R^* \rangle$ of the excited state (2.186MeV), which was 2.276 fm. The estimated root mean square value calculated for ^{6}Li was 2.51 for the ground state [11]. The root mean square (rms) radius $\langle R^* \rangle$ of the excited state (2.186MeV) obtained from α+^{6}Li is 2.959 fm. For the α+^{6}Li. The obtained value of the rms radius of the excited state (2.19 MeV) by averaging the data on both reactions was found to be < R > = 2.86 fm.

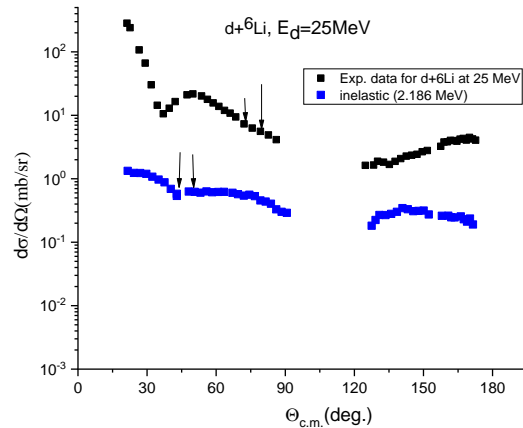**Fig. (1): Differential cross-sections of the α+^{6}Li at 59 MeV (right panel) [12] and d+^{6}Li at 25 MeV (left panel) [13]. The arrows indicate the positions of the extremes.**

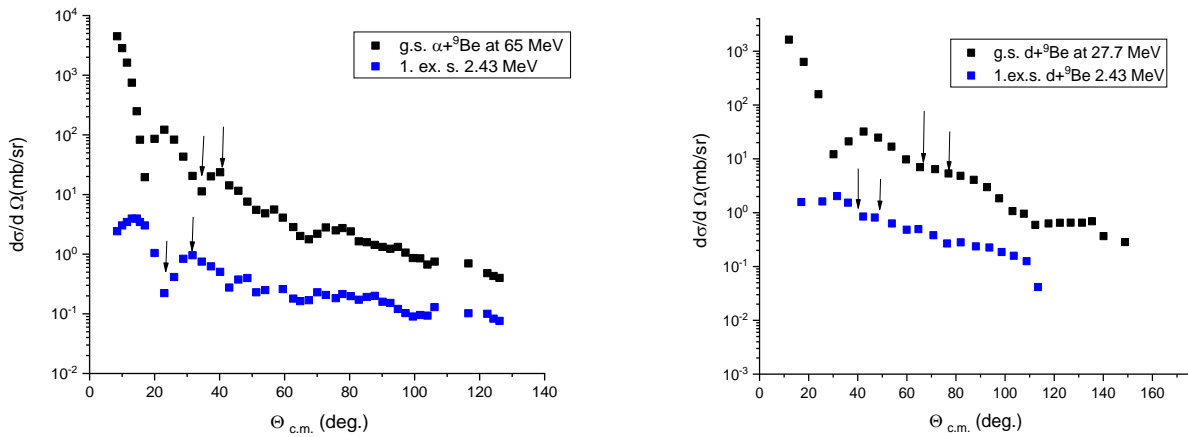**Fig. (2): Differential cross sections of the α+⁹Be and scattering at 65 MeV (left panel) [14] and d+⁹Be at 27.7 MeV (right panel) [15]. The arrows indicate the positions of the extremes.**

The experimental data was used directly to calculate the root mean square (rms) radius $\langle R^* \rangle$ of the excited states as shown in Figs. 1 and 2. The same calculations have been done for d+⁹Be and α+⁹Be at 27.7 and 65 MeV, respectively. The calculated difference R_{dif} (2.19) - R_{dif} (0.00) from d+⁹Be was 0.273 fm, while the rms value of the excited state 2.34MeV of ⁹Be was 2.792 fm. The difference between R^* (the root mean square radius of the excited state) and R_0 (the root mean square radius of the ground state) is equal to 2.519 fm [11], is about 0.251 fm. The difference between R^*_{diff} - R_{diff} from α+⁹Be was 0.42 fm, which is bigger than the obtained value from d+⁹Be, 0.273 fm. The average value obtained for the rms value of the excited state of 2.34 MeV is 2.864 fm. The extracted <R> from alpha scattering is greater than that obtained from deuteron scattering for all of the states discussed here and in previous work [10]. Even the difference between R^*_{diff} - R_{diff} has the same behavior. An important conclusion is that deuteron scattering is more suitable than alpha to be used in this method. All the calculations in the present work have been done using Fresco Code [16].

b. Distance closest approach

Threshold anomaly is a phenomenon where there is a rapid energy variation of the real and imaginary part of the potential in the region around the Coulomb barrier. The strong absorption (imaginary part) appears at a certain distance known as the radial region of sensitivity. The sensitivity of radial distance depends on the bombarding energy for lighter systems. The interaction distance of closest approach for light projectiles ⁶He and ⁶,⁷Li is 2.2 fm, which is higher than the obtained value for stable systems, 1.65 fm [17]. The ratio $d\sigma/d\sigma_{Ruth.}$ has

been used to extract the critical interaction (d_I) and strong absorption (d_s) distances. Where d_I is, the critical interaction distance could be defined as the distance where the elastic cross-section ratio starts deviating from unity and takes the value 0.98. Also, d_s represents the strong-absorption distance. It is the distance where the ratio of elastic scattering to the Rutherford scattering $d\sigma/d\sigma_{Ruth.}$ is equal to 0.25. There is a strong relationship between d_s and the grazing angle $\Theta_{1/4}$ where the ratio of the elastic scattering to the Rutherford scattering is $d\sigma/d\sigma_R = 0.25$ [18]. The distance of the closest approach is given as:

$$D = d\left(A_1^{1/3} + A_2^{1/3}\right) = \frac{1}{2}D_0\left(1 + \frac{1}{\sin\left(\theta_{c.m.}/2\right)}\right), D_0 = \frac{Z_1 Z_2 e^2}{E_{c.m}} \quad (7)$$

where $[Z_1, A_1]([Z_2, A_2])$ correspond to the atomic and mass numbers of the projectile (target), respectively. In order to deduce the reduced interaction distance in a systematic way, the data are fitted with the same exponential growth function of the Boltzmann type:

$$y = \frac{p_1}{1 + e^{-p_2(d - p_3)}} \quad (8)$$

$y = d\sigma/d\sigma_{Ruth.}$ and d is the deduced distance of the closest approach. p_1, p_2, and p_3 are adjustable parameters that were used to fit the experimental data [15]. The closest distance approach has been calculated for d+²⁰⁸Pb as given in Fig.3 agrees with [17]. p_1 was fixed at the unity during the present analysis for all nuclear systems under consideration. The fitting has been done using p_2 and p_3. The closest distance approach for d+²⁰⁸Pb system, the d_s, was 1.40 fm, where d_I is 2.61 fm. The calculations have been done around the Coulomb barrier of the system d+²⁰⁸Pb. It was observed that d_s and d_I obtained for the d+²⁰⁸Pb system are close to ⁶He+⁶⁴Zn as shown in Fig.3 [18, 19]. For the

$\alpha+^{208}$Pb system, the critical interaction distance has been calculated at energies around Coulomb barrier shown in Fig. 3 (left panel). It was observed that the obtained value of d_I is larger in the case of $\alpha+^{208}$Pb than in the case of $d+^{208}$Pb by about 0.26 fm as given in Table 1.

The calculations obtained in the present work give the impression of the similarity between deuteron and ^{6}Li especially at the critical interaction distance as pointed out in [17]. Also, what was observed is that the Fresnel peak observed in the angular distributions under consideration for the ^{4}He+^{208}Pb preventing us to reliably determining the reduced critical interaction distance [19]. It can be observed in Fig. 3 that the reduced strong absorption distance is much smaller for deuteron than for alpha, indicating that

deuteron reaches an inner region in the collision. The distance of the closest approach has been calculated for deuteron and alpha elastically scattered by ^{64}Zn as shown in Fig.3. The obtained parameters in the present analysis are listed in Table 1. The present calculations are compared with those from literature for ^{4}He+^{64}Zn [19] which were in good agreement with literature study. Also, the value of d_s in the case of $d+^{64}$Zn is very small in comparison with alpha particles, which reflects the absorptivity of the deuteron. As presented in Table 1, the absorption for alpha is weaker than deuteron again in the case of the ^{4}He+^{64}Zn system. The d_s value in the case of the $d+^{64}$Zn system listed in Table 1 is half its value in the case of alpha.
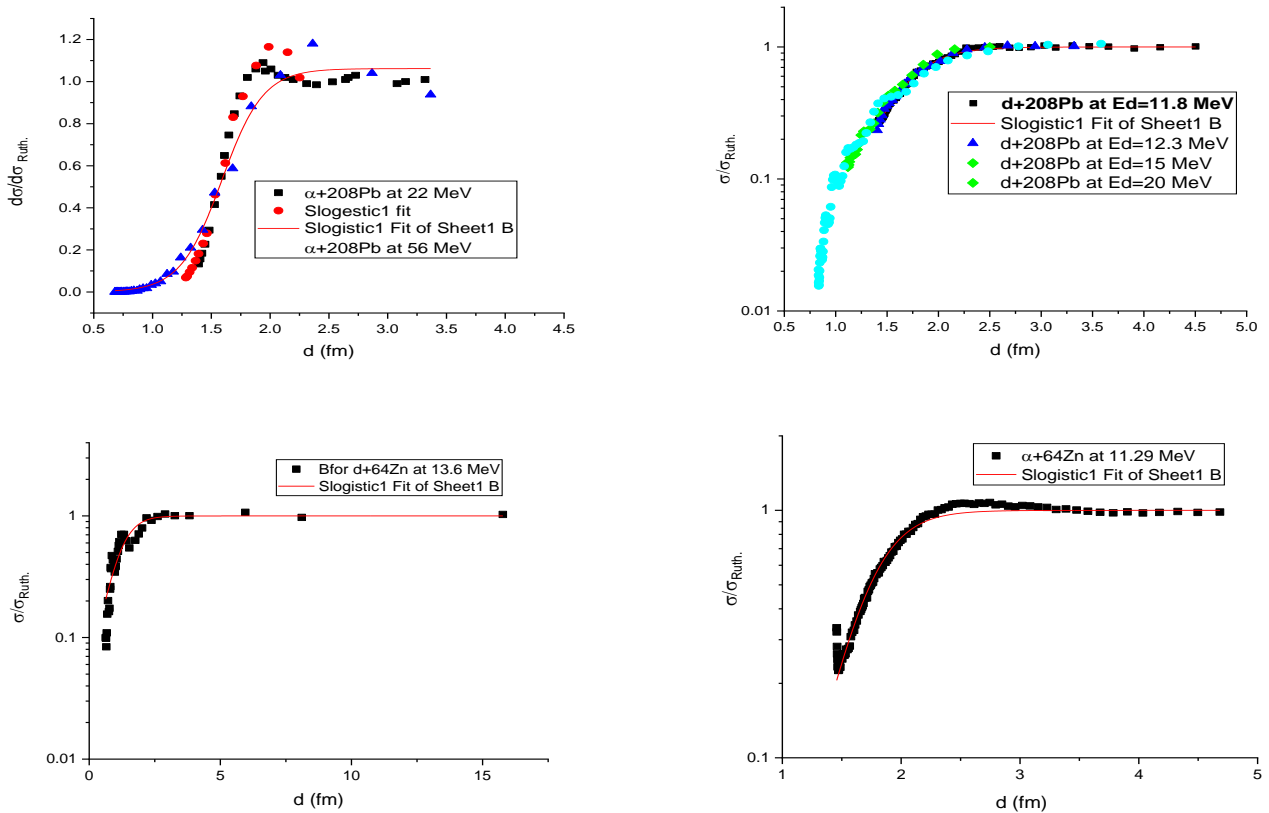

Fig. (3): Ratio of the elastic cross section to the Rutherford value, σ/σ_{Ruth}, as a function of the reduced distance of closest approach for deuteron and alpha elastically scattered by ^{64}Zn [20, 21] and ^{208}Pb [22, 23]

Table (1). The reduced critical interaction distance, d_I, and the reduced strong-absorption distance, d_S (at which $d\sigma/d\sigma_{Ruth}$ is 0.98 and 0.25, respectively), for the systems indicated on deuteron and α elastic scattering by ^{208}Pb and ^{64}Zn

system	d_I	d_s	p_1	p_2	p_3	Ref.
$d+^{208}$Pb	2.477	1.569	1.00	-7.892	1.708	p.w.
$\alpha+^{208}$Pb	2.610	1.480	1.00	-5.642	1.585	p.w.
$\alpha+^{64}$Zn	2.28	1.598	1.019	-4.350	1.856	[19]
$\alpha+^{64}$Zn	2.358	1.512	1.00	-4.777	1.740	p.w.
$d+^{64}$Zn	2.755	0.740	1.00	-2.474	1.177	p.w.

c. Notch test

The conclusion from the previous section pushed us to perform a notch test of the OM potentials for d, α+^{208}Pb scattering systems looking for the region of their sensitivity. The principle of the notch technique is to introduce a localized perturbation into either the real or imaginary radial potential, or move the notch radially through the potential to investigate the influence arising from this perturbation on the predicted cross section [16]. The nuclear potential is defined as:

$$U_N = V(r) + iW(r) = -V_0 f_V(r) - iW_0 f_W(r) \quad \textbf{(9)}$$

where the V_0 and W_0 are depths of the real and imaginary parts of the potential with Woods-Saxon form $f_i(r,a,R)$,

$$f_i(r, a, R) = \left[1 + \exp\left(\frac{r - R_i}{a_i}\right)\right]^{-1}, i = V, W \quad \textbf{(10)}$$

where $R_i = r_{0i}(A^{1/3}_p + A^{1/3}_t)$, A_p and A_t represent the mass numbers of the projectile and target, respectively. Taking the real potential V(r) as an example, the perturbation of the potential V_{notch} can be expressed as:

$$V_{notch} = dV_0 f_V(R', a, R) f_{notch}(r, a', R') \quad \textbf{(11)}$$

where R′ and a′ represent the position and width of the notch, d is the fraction by which the potential is reduced, and f_{notch} (r, a′, R′) is the derivative Woods-Saxon surface form factor:

$$f_{notch}(r, a', R') = 4\exp\left(\frac{r - R'}{a'}\right) / \left[1 + \exp\left(\frac{r - R'}{a'}\right)\right]^2 \quad \textbf{(12)}$$

Thus the perturbed real potential $V_{pert.}(r)$ is [16]:

$$V(r)_{pert.} = V_0 f_V(r, a, R) - V_{notch} \quad \textbf{(13)}$$

The perturbation of the imaginary potential can be derived by the same procedure. The typical perturbed

potential with $r_0 = 1.25$ fm, a = 0.65 fm, R̀= 10 fm, à=0.1 fm, R=1.25($A_p^{1/3}$+$A_T^{1/3}$), and d=1.0 is shown in Fig. 4. Then the dip is moved across the potential, and the relative change of χ^2 is plotted as a function of the reduced radius r. The radial sensitivity of elastic scattering for deuterons and α has been achieved by comparison using the notch test. The notch test has been applied to d+^{208}Pb at 110 MeV and α+^{208}Pb at 288 MeV as shown in Fig. 5. The results plotted in Figs. 5 show that the sensitive region of the deuteron extends well into the surface up to a reduced radius of 2 fm, with the most sensitive region close to the strong absorption radius. The radial sensitivity appears in the case of the deuteron earlier than in the case of alpha as shown in Fig. 5 (left panel). Where the notch test has been applied to α+208Pb at 288 MeV, the radial sensitivity starts at 9 fm. It is observed that deuteron goes closer to the target (^{208}Pb) than in the case of alpha as discussed in the previous section. The obtained result from the notch test agrees with that extracted from the phenomenological method in the previous section.
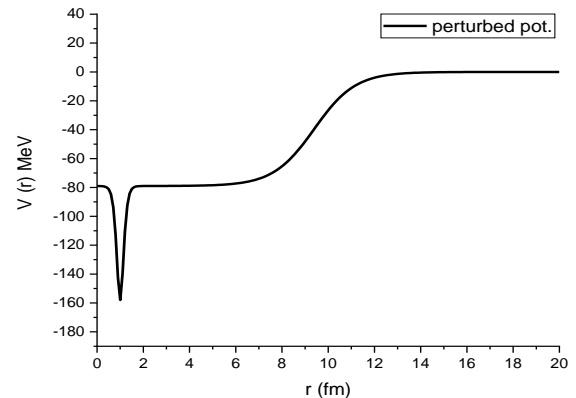

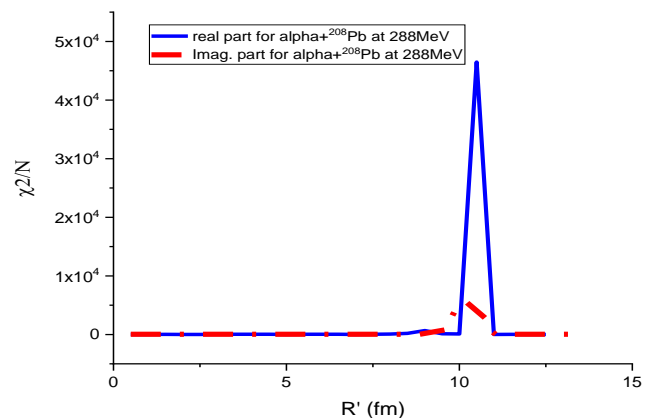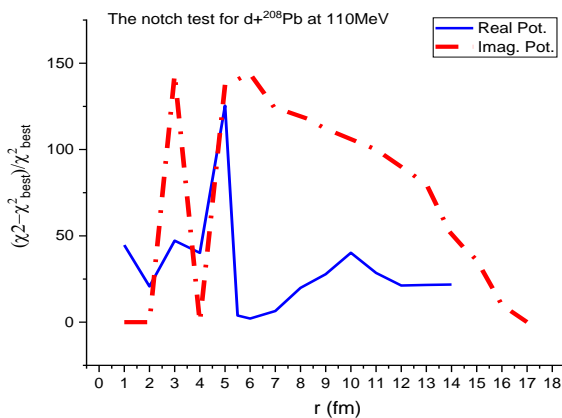**Fig. (4): The typical perturbed potential with $r_0 = 1.25$ fm, a = 0.65 fm, R̀= 1 fm, à=0.1 fm, and d=1.0 where r=R̀**

Fig. (5):. Radial sensitivity for d+^{208}Pb at 110MeV [24] (left panel) and α+^{208}Pb systems 288 MeV [25] right panel.

d. Reduced cross section approaches for a comparison between alpha and deuteron

The choice of the targets ^{6}Li, ^{7}Li, ^{9}Be and ^{11}B was done because we have made the calculations in the ref. [2, 7] which could be used here. The total reaction cross sections is an important piece of information that can be obtained from elastic scattering. The deduced total reaction cross section σ_{reac} for the deuteron and alpha elastically scattered by ^{6}Li, ^{7}Li, ^{9}Be and ^{11}B are respectively shown in Fig. 6. The reaction cross section has been obtained from output of the fresco code [16]. The obtained reaction cross section for ^{2}H and ^{4}He elastically scattered light nuclei were found to be in satisfactory agreement with the predictions obtained in the previous study [26, 27]. The behavior of the calculated total cross section was found to be projectile dependent [27-30]. There are various approaches to re-normalizing the total reaction cross section for the systems under discussion. Re-normalizing the energy and cross sections can be done using the following two equations [31]:

$$E_{red} = E \times \frac{A_P^{\frac{1}{3}}+A_T^{\frac{1}{3}}}{Z_P Z_T}, \qquad (14)$$

$$\sigma_{red} = \frac{\sigma_C}{\left(A_P^{\frac{1}{3}}+A_T^{\frac{1}{3}}\right)^2} \qquad (15)$$

where Z_P (Z_T) is the charge of the projectile (target) and A_P (A_T) is the mass of the projectile (target), and the total reaction cross section is represented by σ_c. The reduction approach was applied to the various systems of the deuteron and alpha elastically scattered by ^{6}Li, ^{7}Li, ^{9}Be and ^{11}B which are shown in Fig. 6. It is observed that a larger reduced total reaction cross sections are obtained at energies around the Coulomb barrier for the deuteron projectile followed by the tightly-bound nuclei alpha, which produces the smallest total reaction cross section [32].

A comparison between the reduced cross section for deuteron and another for alpha should be done at the same reduced energy. At a reduced energy of 10.52MeV, the calculated reduced cross section for ^{6}Li(^{4}He,^{4}He)^{6}Li is 64.5 mb, whereas for ^{6}Li(d,d)^{6}Li, the calculated reduced cross section is 107.2mb, which is much greater in the case of duteron than calculated from alpha under the same conditions. Also, for deuteron and alpha at 10 MeV elastically scattered by ^{7}Li, the reduced cross section was 79.40 mb in the case of ^{7}Li (^{4}He,^{4}He) ^{7}Li and was 100.75 mb in the case of ^{7}Li(d,d)^{7}Li as shown in Fig. 6. The same comparison has been done for alpha and deuteron elastically scattered ^{9}Be and ^{11}B and the same results have been observed (see Fig. 6).
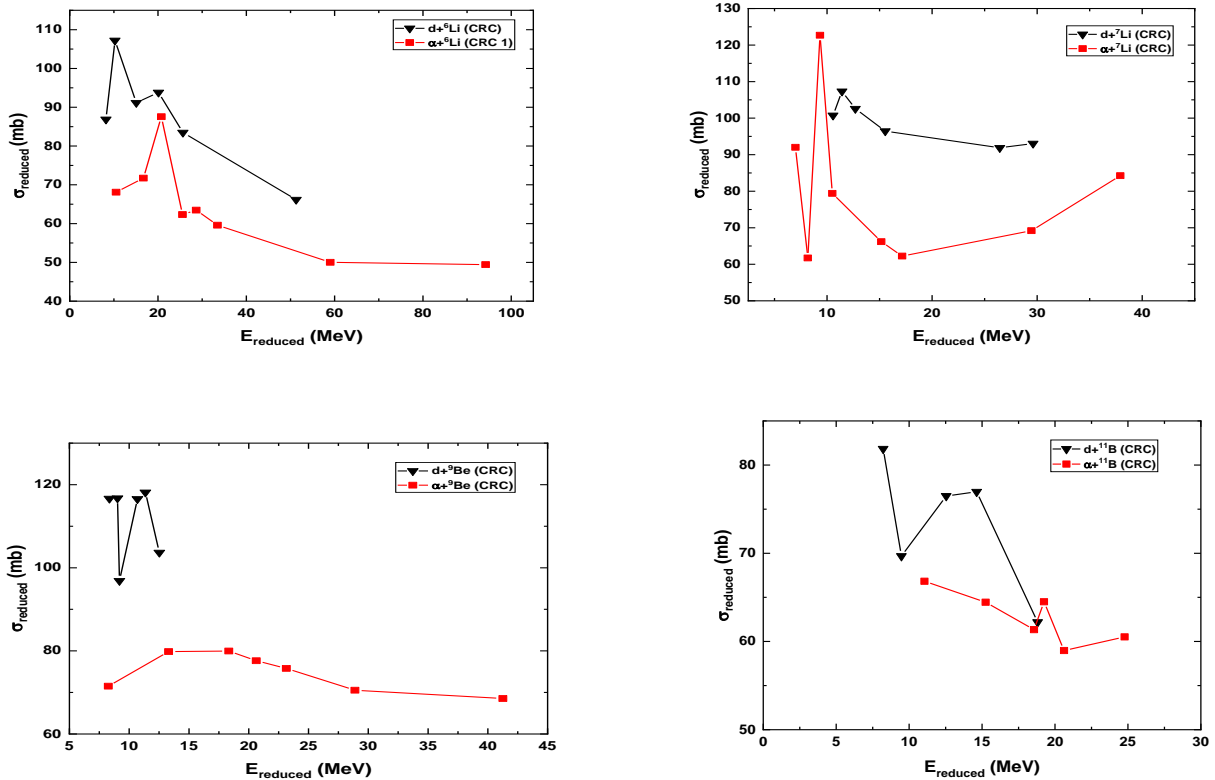

Fig. (6): Reduced reaction cross sections $\sigma_{red.}$ versus reduced energy $E_{red.}$ for deuteron and alpha elastically scattered by ^{6,7}Li, ^{9}Be, and ^{11}B respectively.

It was observed that the calculated total cross section (σ_R) is energy dependent, OMPs dependent, projectile (and/or target) dependent and has also been adjusted using spectroscopic factors in the case of the transfer [7, 31]. As the reduced cross sections for the all nuclear systems under consideration have been obtained from the same author [2, 7], it may be a reliable analysis. It is clear from the Fig. 6 that the reduced cross sections for the deuteron elastically scattered by ^{6,7}Li, ^{9}Be, and ^{11}B are higher than those from alpha with the same nuclei. It demonstrates that the deuteron can be viewed as a halo nuclei, with the proton in the center and the neutron rotating around it. *Now, it is concluded that the deuteron has a signature of a halo nucleus.*

e. Reflexion coefficients η_L for deuteron and alpha elastically scattered by ^{6,7}Li, ^{9}Be and ^{11}B

For a comparison between deuteron and alpha elastically scattered by ^{6}Li, ^{7}Li, ^{9}Be and ^{11}B, we presented Figs. 7-14 for the reflexion coefficients, η which are related to the scattering matrix S_L by the simple known relation:

$$S_L = \eta_L \times exp(2i\delta_L) \qquad (16)$$

where the reflexion coefficients η_L and the phase shifts δ_L are real. Usual behavior for deuteron and alpha elastically scattered by ^{6}Li, ^{7}Li, ^{9}Be and ^{11}B has been detected for η_L close to zero at small angular momenta L (total absorption), increasing η_L for intermediate L (partial absorption), and when η_L close to unity (no absorption) for large L. For all systems, deuteron and alpha elastically scattered by ^{6}Li, ^{7}Li, ^{9}Be and ^{11}B, the slopes of η_L are different. The derivative $\frac{d\eta}{dL}$ is one

choice to compare between all systems under consideration from the width ΔL at the same energies as shown in Figs. 7-14.

Significant differences were detected between the two projectiles, alpha and deuteron, elastically scattered by light nuclei with the maximum slope $d\eta_L/dL$ at the angular momentum L_0 and the width ΔL at full width at half maximum value (FWHM). For the deuteron, the width ΔL is larger than that calculated from alpha. The widths of the two curves at the same reduced energy show a signature of the effect of the neutron halo on deuterons. For example, in the case of alpha elastically scattered by ^{6}Li, the width ΔL at $E_{red.}$ 25 MeV was 1.867, whereas for the deuteron with the same conditions it was 2.4376. The calculated width ΔL for alpha, elastically scattered by ^{9}Be at $E_{red.}$ 8.25 MeV is 1.417 whereas it is 2.466 at $E_{red.}$ 8.35 MeV in the case of deuteron. There are many examples that could be taken from such an argument for ^{7}Li and ^{11}B. The derivative $d\eta_L/dL$, obtained from [2] and [7], for deuteron and alpha elastically scattered by ^{6}Li, ^{7}Li, ^{9}Be and ^{11}B at the energies below and close to the Coulomb barrier, is presented in Figs. 7-14 for all cases under consideration. The maximum derivative $(d\eta_L/dL)_{max}$, position L_0 of the maximum derivative $d\eta_L/dL$ and the Gaussian width ΔL (FWHM) of $d\eta_L/dL$ for deuteron and alpha elastically scattered by ^{6}Li, ^{7}Li, ^{9}Be and ^{11}B were obtained from Figs. 7-14. The increase in ΔL values at the $d\eta_L/dL$ vs. L curve (see Figs. 7–14) was taken as a signature of the halo properties of the deuteron projectile [6, 21]. A Gaussian fitting of the derivatives $d\eta_L/dL$ as a function of angular momentum for all the systems under consideration, as shown in Figs. 7–14.
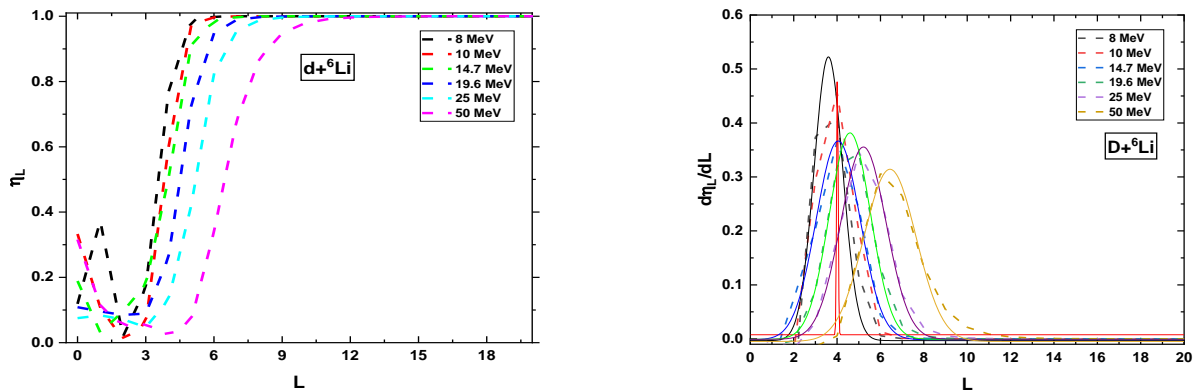

Fig. (7): Reflexion coefficients η_L for ^{6}Li (^{2}H, ^{2}H) ^{6}Li at E_{lab} = 8−50 MeV (left panel) and the derivatives $d\eta_L/dL$ (right panel).
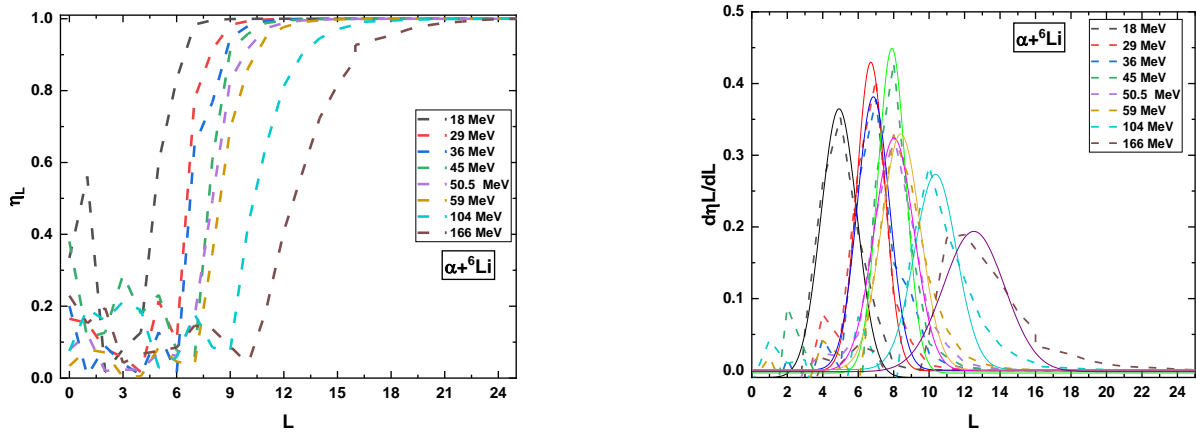
Fig. (8): Reflexion coefficients η_L for ^{6}Li (^{4}He, ^{4}He) ^{6}Li at E_{lab} = 18−166 MeV (left panel) and the derivatives $d\eta_L/dL$ (right panel).
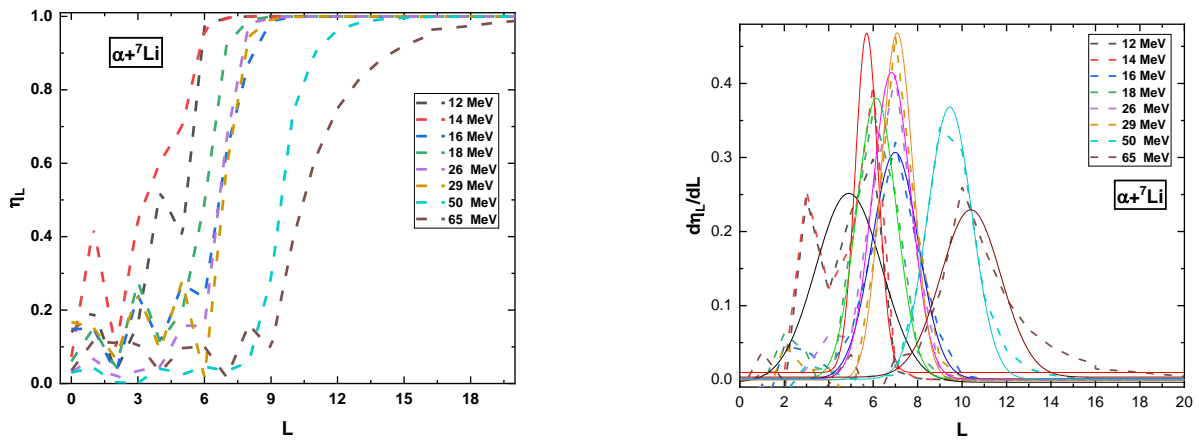
Fig. (9): Reflexion coefficients η_L for ^{7}Li (^{4}He, ^{4}He) ^{7}Li at E_{lab}= 10−28MeV (left panel) and the derivatives $d\eta_L/dL$ (right panel).
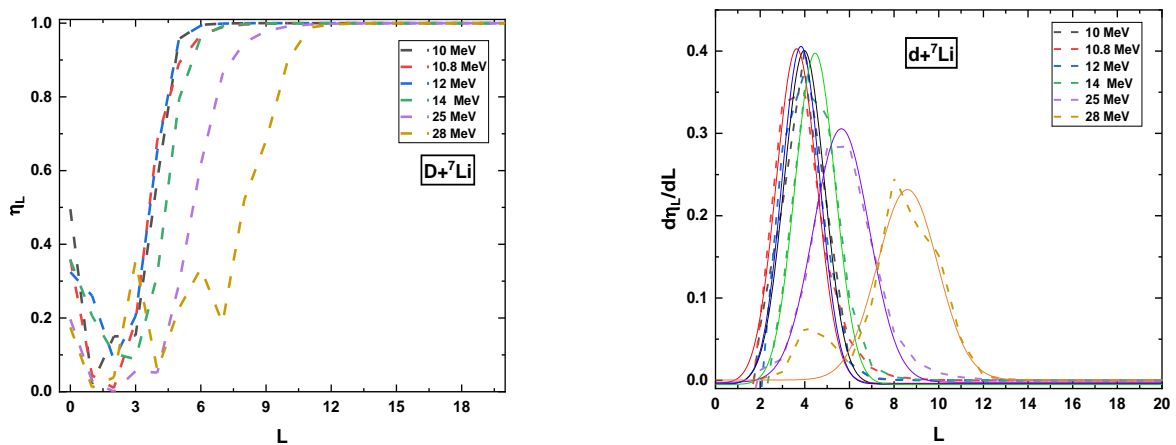
Fig. (10): Reflexion coefficients η_L for ^{7}Li(^{2}H, ^{2}H)^{7}Li at E_{lab}= 18−166 MeV (left panel) and the derivatives $d\eta_L/dL$ (right panel).
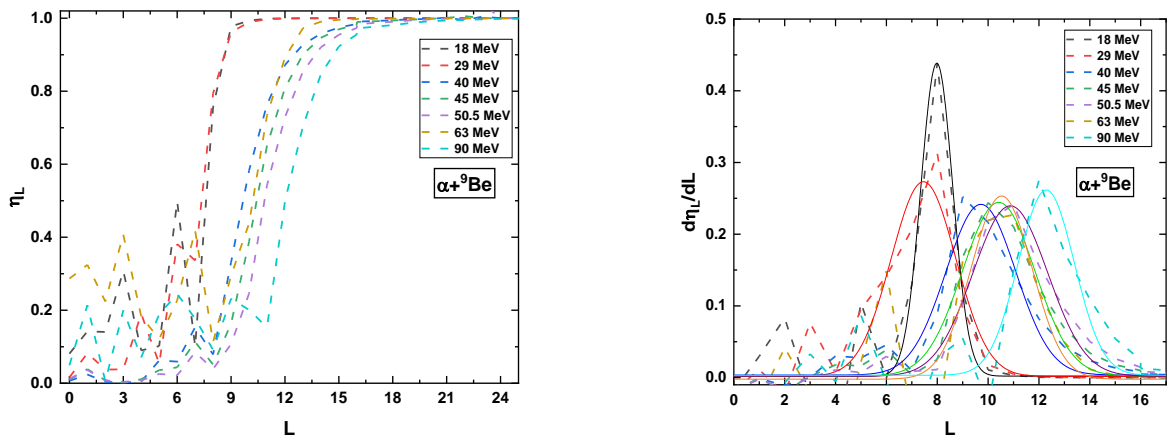
Fig. (11): Reflexion coefficients η_L for ^{9}Be(^{4}He, ^{4}He) ^{9}Be at E_{lab}= 18−90MeV (left panel) and the derivatives $d\eta_L$/dL (right panel).
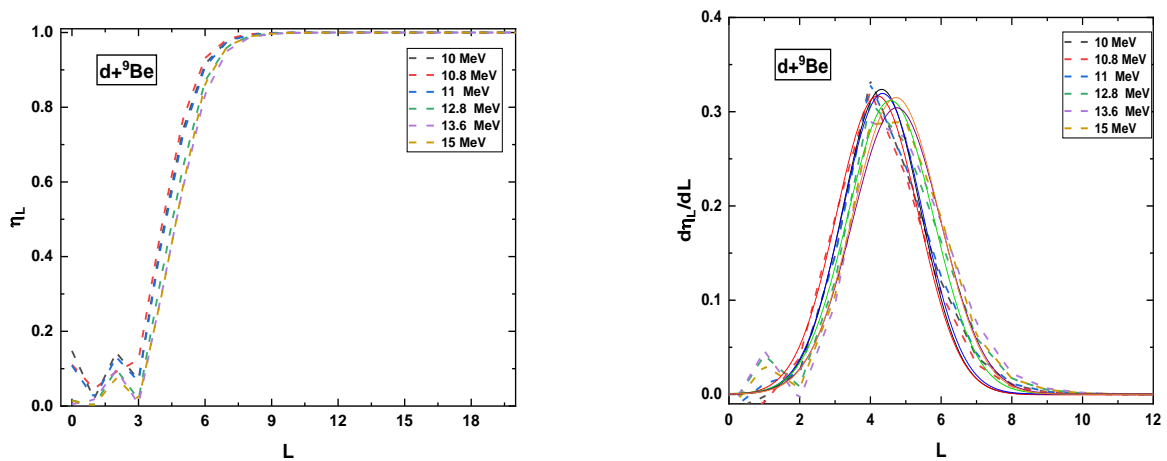
Fig. (12): Reflexion coefficients η_L for ^{9}Be(^{4}He, ^{4}He) ^{9}Be at E_{lab}= 18−90MeV (left panel) and the derivatives $d\eta_L$/dL (right panel).
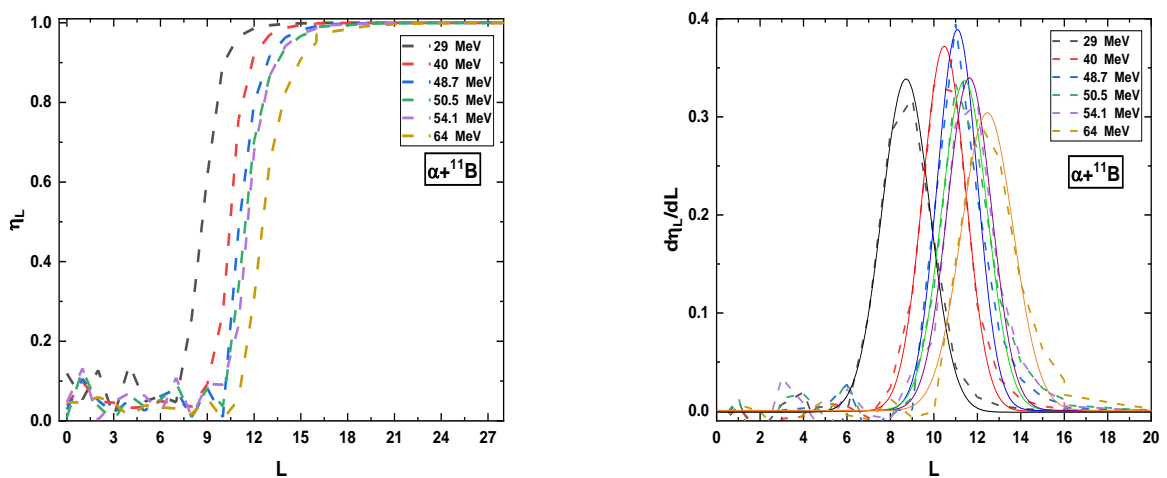
Fig. (13): Reflexion coefficients η_L for ^{11}B(^{4}He, ^{4}He) ^{11}B at E_{lab}= 29−64 MeV (left panel) and the derivatives $d\eta_L$/dL (right panel).
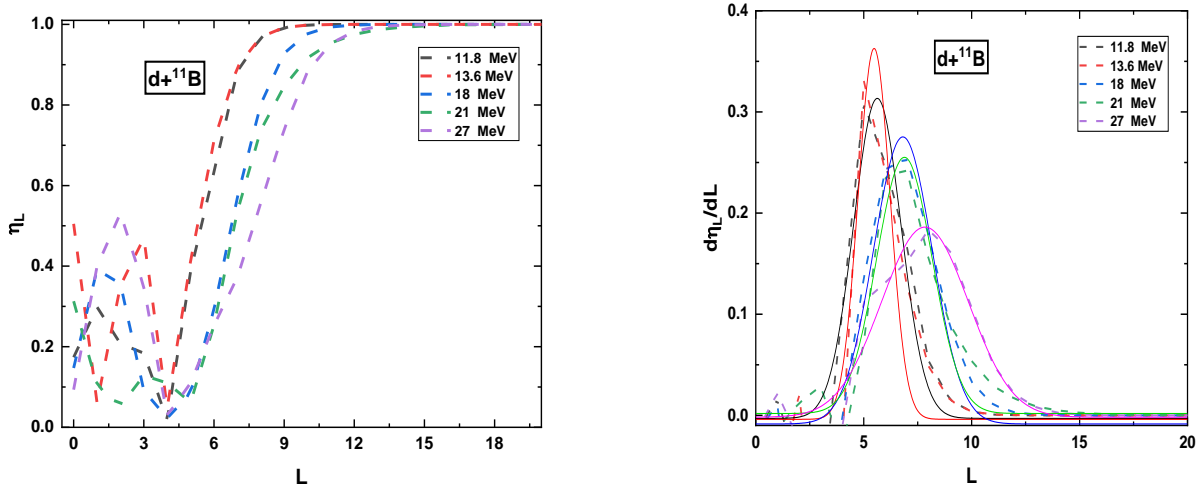
Fig. (14): Reflexion coefficients η_L for ¹¹B(²H, ²H) ¹¹B at E_lab= 11−27MeV (left panel) and the derivatives dη_L/dL (right panel).

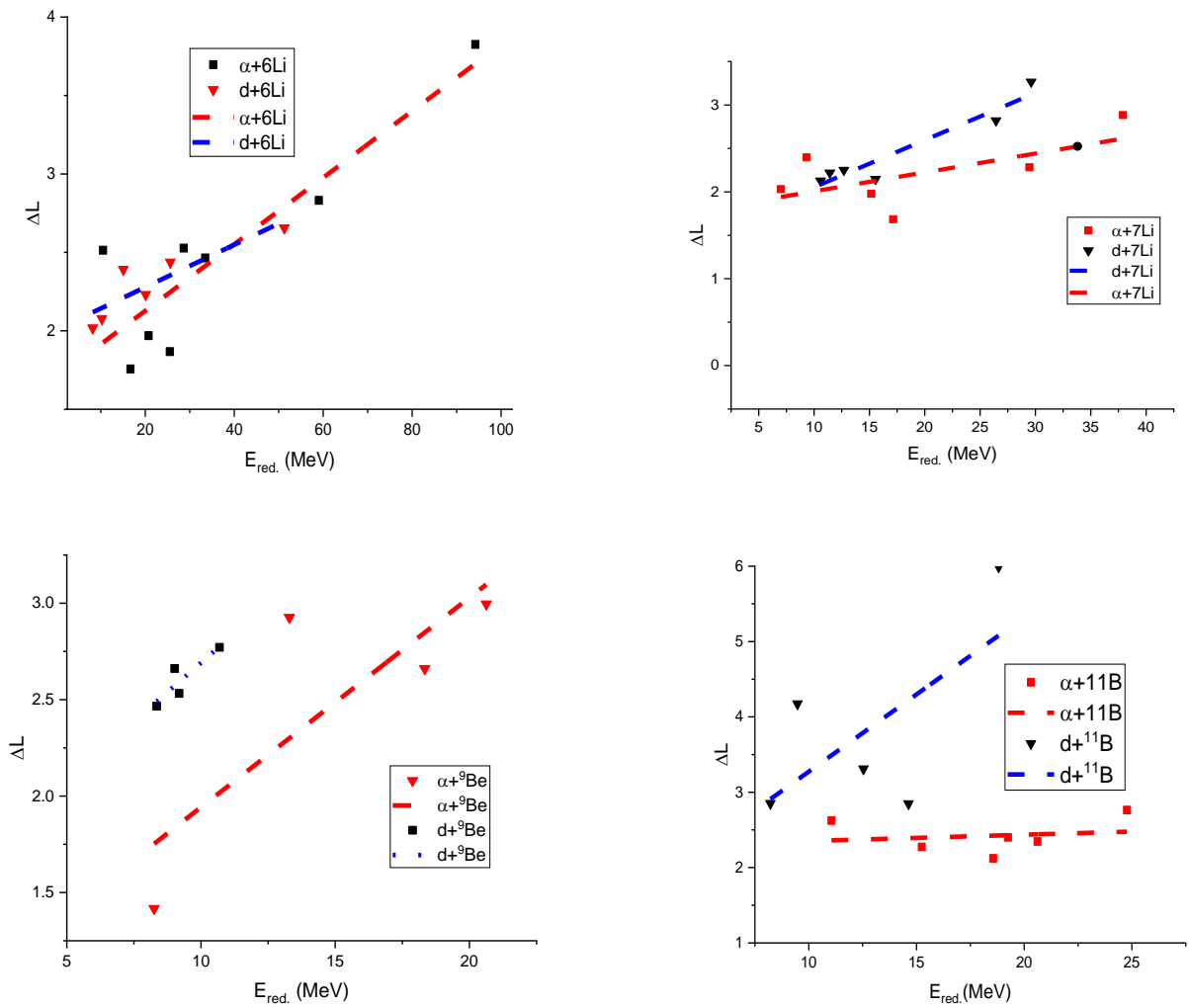**Fig. (15): The Gaussian width ΔL of dη_L/dL derivatives versus the reduced energy E_red. for all the considered nuclear systems**
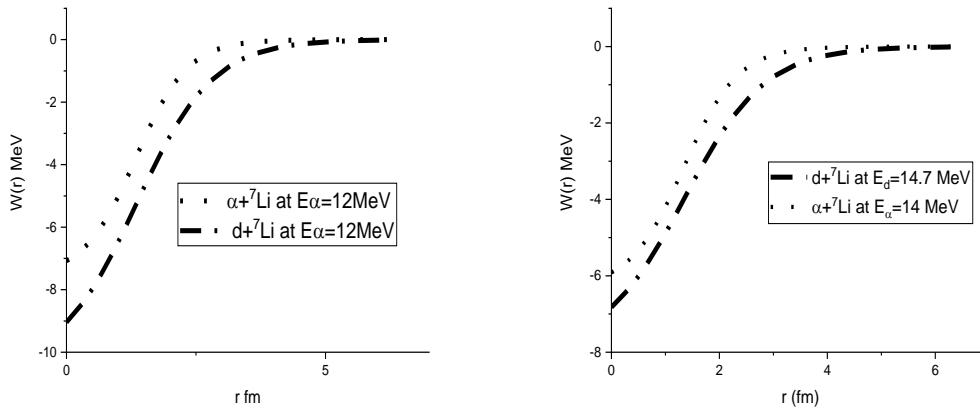
**Fig. (16): A comparison between the imaginary potentials for deuteron and alpha elastically scattered by
^{7}Li where the dash line represents α+^{7}Li [7] and the dashed lines represents d+^{7}Li [2] (the same
energy was used during the analysis)**

Fig. 15 depicts the position L_0 of the maximum derivative $(d\eta_L/dL)_{max}$ for the all considered systems versus the reduced energy $E_{red.}$ and the Gaussian width ΔL of versus the reduced energy $E_{red.}$. From this analysis, it can be concluded that the deuteron elastically scattered by ^{6,7}Li, ^{9}Be and ^{11}B shows an increasing width ΔL at higher energies. We get deuteron and alpha elastically scattered by ^{7}Li shown in Fig. 15, that:

$$\frac{\Delta(\Delta L)}{\Delta E_{red.}} \approx 0.5428/MeV \quad for\ deuteron \qquad (17)$$

$$\frac{\Delta(\Delta L)}{\Delta E_{red.}} \approx 0.383/MeV \quad for\ alpha \qquad (18)$$

Only one example has been discussed because all the systems under consideration are similar to each other, as shown in Fig.15.

Only the discrepancy appears in the case of deuteron elastically scattered by ^{6}Li as shown in Fig. 15 which reflects the cluster structure of ^{6}Li≡d+α. The structure of ^{6}Li is responsible for such behavior of ΔL of $d\eta_L/dL$ derivatives versus the reduced energy $E_{red.}$

A comparison between the imaginary potentials for deuteron and alpha elastically scattered by light nuclei

Another method for comparing deuteron and alpha elastically scattered by light nuclei has been proposed here, using the behavior of imaginary part W(r) for both systems at the same energies. An example has been chosen for deuteron and alpha elastically scattered by ^{7}Li at 12 MeV and 14 MeV, as shown in Fig.16 (just a case for a comparison). It is observed from Fig. 16 that the deuteron has a deeper imaginary potential than in the

case of alpha, which reflects more absorptivity in the case of the deuteron.

3- CONCLUSIONS

The diffraction model has been applied to deuteron and alpha, elastic and inelastic scattering, to extract the radius of the ground and excited states. The model has been applied to ^{6}Li, ^{9}Be and ^{11}B where the projectiles were alpha and deuteron. The <R> obtained from alpha scattering is greater than that obtained from deuteron scattering in both the current study and the literature. It is concluded that deuteron scattering is more suitable than alpha to be used in the diffraction model. The interaction distance of the closest approach for light nuclei projectiles, deuteron and alpha, near the Coulomb barrier has been calculated using the phenomenological method for the targets, ^{64}Zn and ^{208}Pb. It was observed that the deuteron reaches an inner region in the collisions with ^{64}Zn and ^{208}Pb targets. In contrast to the properties of alpha and deuteron (tightly and weakly bound nuclei), the absorption is weaker for alpha than for deuteron. To draw a complete picture of deuteron and alpha, the notch test technique has been applied to d+^{208}Pb at 110 MeV and α+^{208}Pb system at 288 MeV. As was observed, deuteron goes closer to the target (^{208}Pb) than in the case of alpha, which agrees with the conclusion obtained from the extracted distance of the closest approach. Both the notch test and the distance of the closest approach produce the same result.

To obtain more information about the deuteron and alpha in the present comparison, reduced cross section approaches have been used. The calculated cross section for deuteron elastically scattered by ^{6,7}Li, ^{9}Be,

and [11]B are higher than that of alpha, which indicates that *deuteron is a halo nucleus from the comparison with alpha particles.* Reflexion coefficients have been used during the comparison between deuteron and alpha. It could be concluded that deuteron elastically scattered by [6,7]Li, [9]Be and [11]B shows an increasing width ΔL at higher energies. The calculated value of $\frac{\Delta(\Delta L)}{\Delta E_{red.}} \approx 0.5428/MeV$ for deuteron where it was $0.383/MeV$ for alpha at the same energy, which is taken as a signature of the halo properties of the deuteron.

One method for comparing the deuteron and alpha is the behavior of imaginary part, W(r) for alpha and deuteron elastically scattered by [7]Li at the same energy. The imaginary potential in the case of deuteron is deeper than in the case of alpha, which reflects more absorptivity of the deuteron nucleus. The depth of the real part of the optical potential in the case of an alpha projectile was twice its value in the case of a deuteron.

REFERENCES

[1] S. Lukyanov et al., "Cluster Structure of [9]Be from [3]He+ [9]Be Reaction," in Journal of Physics: Conference Series, 2016, vol. 724, no. 1, p. 012031: IOP Publishing.

[2] A. Amar and A. A. Ibraheem, "Elastic scattering of light nuclei by deuterons with different models," J International Journal of Modern Physics E, vol. 30, no. 10, pp. 2150090-172, 2021.

[3] A.H. Wapstra, G. Audi, and C. Thibault. Nuclear Physics A729, 129 (2003).

[4] G. Audi, A.H. Wapstra, and C. Thibault. Nuclear Physics A729, 337 (2003).

[5] Jin Lei and Antonio M. Moro arXiv:2305.14111v1 [nucl-th] 23 May 2023.

[6] P. Mohr et al., "Comparison of [120]Sn ([6]He, [6]He) [120]Sn and [120]Sn (α, α) [120]Sn elastic scattering and signatures of the [6]He neutron halo in the optical potential," J Physical Review C, vol. 82, no. 4, p. 044606, 2010.

[7] A. Amar, "Analysis of alpha elastically scattered by light nuclei applying different models," J International Journal of Modern Physics E, vol. 31, no. 02, p. 2250011, 2022.

[8] Y. A. Berezhnoy, V. YU. KORDA, and A. Gakh, "Matter-density distribution in deuteron and diffraction deuteron-nucleus interaction," J

[9] https://www-nds.iaea.org/exfor/.

[10] A. Demyanova, A. Ogloblin, A. Danilov, T. Belyaeva, and S. Goncharov, "Radii of cluster states in 11 B and 13 C," J International Journal of Modern Physics E, vol. 20, no. 04, pp. 915-918, 2011.

[11] B. A. Brown, C. Bronk, and P. Hodgson, "Systematics of nuclear RMS charge radii," J Journal of Physics G: Nuclear Physics, vol. 10, no. 12, p. 1683, 1984.

[12] F. Foroughi, E.Bovet, and Ch. Nussbaum, J. Phys.G 5, 1731 (1979).

[13] N. Burtebayev, J.T. Burtebayeva, A. Duisebayev, Zh.K. Kerimkulov , M. Nassurlla, T. Zholdybayev, S.V. Artemovb , A.A. Karakhodzhayevb , U.S. Salikhbayevb S.B. Sakutac , S. Kliczewskid , E. Piaseckie , K. Ruseke R. Siudakd , A. Trzcińskae , M. Wolińska-Cichockae , A. Amar, Acta Physica Polonica B, No 5, Vol. 46 (2015).

[14] S. Roy, J.M. Chatterjee, H. Majumdar ,S.K. Datta, S.R. Banerjee, S.N. Chintalapudi, Phys. Rev. C 52,1524,1995.

[15] R.J. Slobodrian, Nucl. Phys. A 32, 684, 1962.

[16] I. Thompson, Fresco 2.0, Department of Physics, University of Surrey, Guildford GU2 7XH, England, 2006.

[17] A. Pakou and K. Rusek, "Interaction distances for weakly bound nuclei at near barrier energies," J Physical Review C, vol. 69, no. 5, p. 057602, 2004.

[18] P. Nistal, V. Guimarães, and J. Lubian, "Distance analysis of elastic scattering data of light projectiles on [27]Al target," in Journal of Physics: Conference Series, 2022, vol. 2340, no. 1, p. 012038: IOP Publishing.

[19] V. Guimaraes et al., "Role of cluster configurations in the elastic scattering of light projectiles on [58]Ni and [64]Zn targets: a phenomenological analysis," J The European Physical Journal A, vol. 57, no. 3, pp. 1-13, 2021.

[20] R.K. Jolly, M.D. Goldberg, A.K. Sengupta, J,NPA,123,54,1969.

[21] A. Ornelas et al., "α scattering and α-induced reaction cross sections of [64]Zn at low energies," Physical Review C, vol. 94, no. 5, p. 055807, 2016.

[22] T. Murayama, Y. Tagishi, T. Sakai, M. Tomizawa, H. Nishikawa, S. Seki, J,NP/A,486,(2),261,198809.

[23] A.M. Baxter, S. Hinds, R.H. Spear, T.H. Zabel, R. Smith, Nucl. Phys. A 369, 25, 1981.

[24] A. Betker, C. A. Gagliardi, D. Semon, R. E. Tribble, H. Xu, and A. Zaruba, "Deuteron elastic scattering at 110 and 120 MeV," J Physical Review C, vol. 48, no. 4, p. 2085, 1993.

[25] B. Bonin et al., "Alpha-nucleus elastic scattering at intermediate energies," J Nuclear Physics A, vol. 445, no. 3, pp. 381-407, 1985.

[26] M.-E. Brandan and G. R. Satchler, "The interaction between light heavy-ions and what it tells us," J Physics reports, vol. 285, no. 4-5, pp. 143-243, 1997.

[27] M. Takechi et al., "Reaction cross sections at intermediate energies and Fermi-motion effect," J Physical Review C, vol. 79, no. 6, p. 061601, 2009.

[28] D. Brink and G. Satchler, "The role of the attractive nuclear potential in determining reaction cross sections," J Journal of Physics G: Nuclear Physics, vol. 7, no. 1, p. 43, 1981.

[29] C.-C. Sahm et al., "Total reaction cross section for ^{12}C on ^{12}C, ^{40}Ca, ^{90}Zr, and ^{208}Pb between 10 and 35 MeV/nucleon," J Physical Review C, vol. 34, no. 6, p. 2165, 1986.

[30] M. Atkinson and W. Dickhoff, "Investigating the link between proton reaction cross sections and the quenching of proton spectroscopic factors in ^{48}Ca," J Physics Letters B, vol. 798, p. 135027, 2019.

[31] P. Gomes, J. Lubian, I. Padron, and R. Anjos, "Uncertainties in the comparison of fusion and reaction cross sections of different systems involving weakly bound nuclei," Physical Review C, vol. 71, no. 1, p. 017601, 2005.

[32] J. Kolata and E. Aguilera, "Interaction barriers for light, weakly bound projectiles," J Physical Review C, vol. 79, no. 2, p. 027603, 2009.